1-kw Arcjet-Engine System-Performance Test

ADRIANO C. DUCATI,* HAROLD HUMPAL,† JOSEPH MELTZER,‡ ERICH MUEHLBERGER,§ JAMES P. TODD,¶
AND HERMAN WALTZER**
Giannini Scientific Corporation, Santa Ana, Calif.

A 1-kw-d.c. arcjet-engine system (with power conditioning equipment and a cryogenic hydrogen propellant storage unit) was tested at the NASA Lewis Research Center in 1962 at an environmental pressure of 8 × 10^{-5} mm of mercury. This radiation-cooled arcjet engine was designed to operate at approximately 1000-sec specific impulse. Current, voltage, propellant flow rate, thrust, chamber pressure, and body temperatures were measured continuously. Engine efficiencies (10–30%) and specific impulses (600–1400 sec) were deduced from the data, but reliability of the thrust measurements was poor. The exhaust plume was photographed with high-speed infrared film and various filters to reveal the size, turning angle, and shape of various wavelength regions. Plume radiation was measured by a radiometer with identical filters to determine the spectral distribution.

Introduction

The arcjet engine described in this paper was designed for early flight testing of an electrical propulsion system in the Space Electric Rocket Test (SERT) program. Factors that should be evaluated in flight include: 1) effects of arcjet interference with communications, with respect to both transmission and reception of command signals through the arc-generated noise and ionized wake, and radar cross section of the wake; 2) the influence of exhaust jet characteristics (radiation, impingement shape) upon spacecraft design under the hard vacuum of space; and 3) unforeseen effects of true space conditions.

The initial objectives of the SERT program required that the engine be compact (8 in. in diameter and 14 in. long), light (≤ 12 lb), and capable of 24 min of unattended operation in a predictable manner.[1] All of the physical limitations established by the SERT program were met by the Plasmadyne†† 1-kw arcjet engine (Fig. 1). The large vacuum pumping requirements for testing this engine limited the environmental pressures that could be obtained in the NASA Lewis Research Center vacuum tunnel to the order of 10^{-4} mm Hg. The major objectives of this ground-test program[2] included: 1) determination of the effects of vacuum and resulting plume expansion on thrust, specific impulse, efficiency, starting performance, operating temperature, and electrode erosion; 2) determination of the thermal influence of an operating thrustor on all components in the engine pod, particularly the cryogenic propellant supply; 3) performance of a series of start-stops to determine the effect of peak inverse voltage feedback on the power-conditioning equipment and to establish restart capability; and 4) measurements of total radiation gross spectral distribution of radiation, and exhaust plume size and shape.

Received June 18, 1963; revision received March 19, 1964. Engine development and tests were conducted by Giannini Scientific Corporation under Contract NAS 5-651 with NASA.

* Technical Director, Special Projects Group. Member AIAA.

† Presently Section Head, Advanced Power Systems, Aerojet-General Corporation, Azusa, Calif. Member AIAA.

‡ Presently Member of Technical Staff, Aerospace Corporation, El Segundo, Calif. Member AIAA.

§ Research Engineer, Special Projects Group. Member AIAA.

¶ Senior Engineer, Special Projects Group. Member AIAA.

** Presently Research Specialist, Space and Information Systems Division, North American Aviation, Downey, Calif. Member AIAA.

†† Formerly a subsidiary, now part of the Santa Ana Division of Giannini Scientific Corporation.

1-kw Arcjet-Engine System

The basic design of a radiation-cooled 1-kw arcjet engine is described in Ref. 3. For this test, several design changes were made, the most significant being in the starting system. The complete system consists of a thrustor, a cryogenic propellant storage and feed system, starting equipment, power-conditioning equipment, supporting frame, and instrumentation.

The propellant system (Fig. 2) employs a 1-liter Dewar in which the liquid hydrogen is heated either by conduction and radiation from the outer shell or by an electric immersion heater. Hydrogen flow is started only when the fluid is in a supercritical state. After flow is started, tank pressure is maintained by three heat exchangers, one of which is inside the tank. A pressure-operated heat-exchanger control valve causes the hydrogen that has been warmed in the first heat exchanger to recirculate through the inside tank and then to return through the third heat exchanger. The external heat exchangers are bonded to the outer shell of the tank. The hydrogen then passes through a pressure regulator, a final heat controller, and a metering orifice to the thrustor with its pneumatic starting system.[4]

The anode nozzle had a 60° divergence, followed by a short section of high divergence (Fig. 3). The cathode tip geometry was a double cone with narrow flats across the intersection. The thrustor employed a contact start mechanism whereby the arc is initiated as the cathode is retracted from contact with the anode. This action is controlled by a pres-

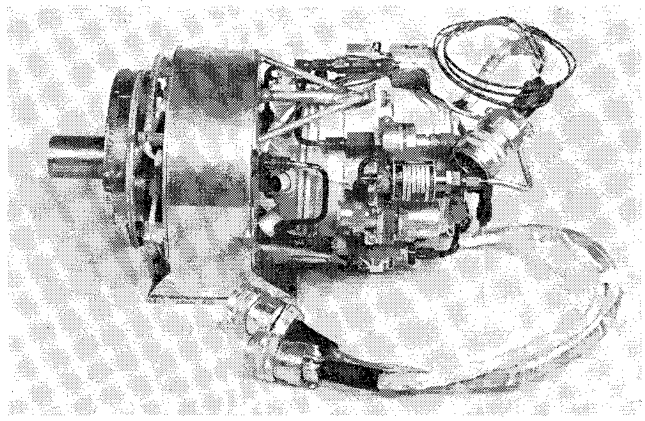

Fig. 1 1-kw arcjet engine.

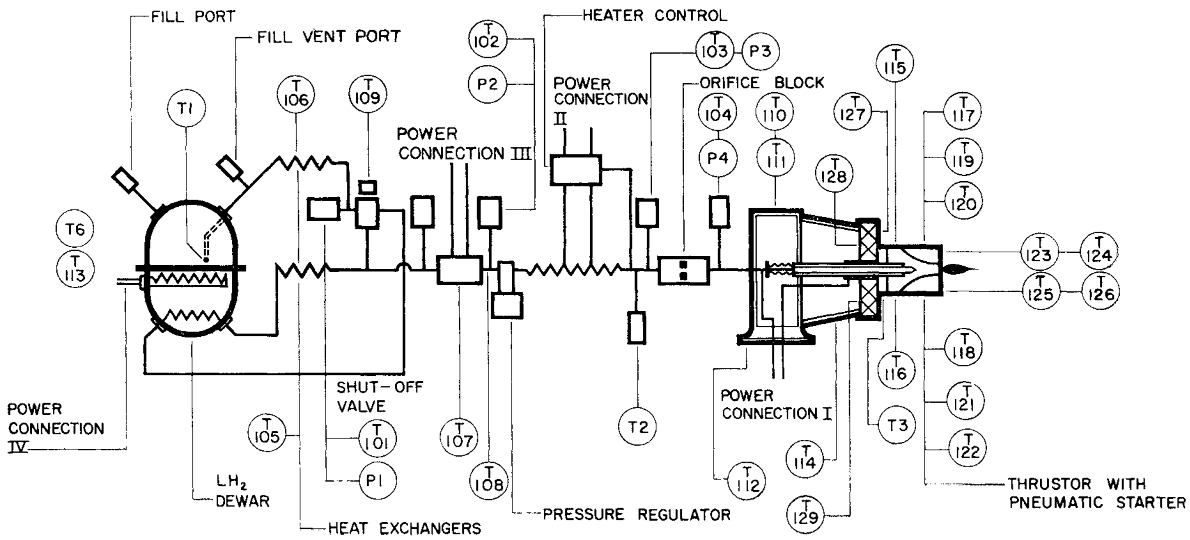

Fig. 2 System instrumentation schematic.

surized bellows. All male threads of mating parts and all sealing surfaces were gold plated to avoid the galling that had occurred between molybdenum parts on earlier models. This proved to be quite valuable when the engines were disassembled for observation after testing. All parts were removed quite easily, and the seals were leak-tight.

The design of the various test-system elements had to be such that testing could be performed in two facilities—a 30-in.-diam, 6-ft-long vacuum test tank atGianni ni Scientific Corp. and a 15-ft-diam, 60-ft-long vacuum tank at NASA Lewis Research Center. The pumping capabilities of these facilities were 10^{-5} lb/sec at 1 mm Hg and at 8×10^{-5} mm Hg, respectively. To insure that the test program would flow smoothly, all engines were made interchangeable. Prior to assembly of each unit, critical parts were inspected. Each supercritical storage system was checked for performance and leak-tightness, the electrical circuit was checked for continuity and resistance to ground, and the cathode bellows operation was timed.

The instrumentation used on this test is shown schematically on Fig. 4. The critical parameters were continuously recorded. A 16-mm movie camera was synchronized with the engine operation. A 35-mm camera was used as a pinhole camera with IR film and filters. The radiometer was equipped with a remote-controlled filter changer and used the same filters as the camera. The sensor attachment points are shown in Fig. 2.

Gaseous hydrogen (20 ppm impurities) was used during checkout periods. Liquid hydrogen was used for all tests that simulated spaceflight conditions; it had a minimum parahydrogen content of 95%, with a maximum impurity content of 40 ppm. At both test facilities, liquid hydrogen was stored in the open. The LSH 150 liquid hydrogen containers (Linde Corp.) leaked enough heat to maintain a 10 psig pressure under withdrawal rates as high as 150 liters/hr, but the flow during the filling of the engine system's tank was higher than could be supported by the heat leak. When the storage vessel pressure dropped much below 10 psig, precooling of the engine's tank was difficult; therefore, the LSH 150 had to be pressurized with helium.

There are three circumstances under which it becomes necessary quickly to empty the supercritical tank of hydrogen: engine malfunction (especially when tank pressure is high), emptying and purging at the end of a test, and leaks in the storage vessel. Therefore, two safety-vent valves were installed in the system to provide for dumping.

All thermal arc-engine power supplies were d.c. and had a similar characteristic in that the $\Delta V/\Delta I$ was made as high as possible. The circuit diagram for the battery cart used at Giannini Scientific Corp. can be found in Ref. 5. At NASA, a 110-v, single-phase transformer rectifier with a series inductance in the secondary and series resistance in the output was used. For the control power to the solenoids, relays, and radiometer, a d.c. supply of 28 $\pm$1.4 v was used.

A thrust-measuring method was sought which would measure 0.010 lb of thrust—considering variations in engine weight and the need for a large number of instrumentation and control lines. A 47-in. double-cantilever beam comprised of two parallel 1-in. tubes, 8 in. apart, was finally selected. The tubes were used as conduits for instrumentation and power leads. The parallel arrangement made the assembly comparatively stiff to transverse loads. The propellant tank was centered on the beam axis, so that propellant weight change would not contribute to beam bending. The calculated beam deflection at the sensing point was 194×10^{-3} in. for 0.010-lb load. The beam deflection was sensed by a Schaevitz differential transformer, the body of which was supported by a much stiffer cantilever beam from the same upper base. The transformer core was tied to the lower end of the support cantilever; this arrangement provided extremely accurate and frictionless measurement of deflection. A permanent magnet was used to damp the cantilever beam, which had a natural frequency of approximately 2.5 cps. A stainless-steel reflector was attached to a third set of supports to prevent radiant heating of the thrustor beam; during a 24-min test, the beam temperature increased 3° F with no detectable gradient front to back. The signal from the differential transformer was amplified and demodulated by a Daytronic amplifier, and the output was fed first through

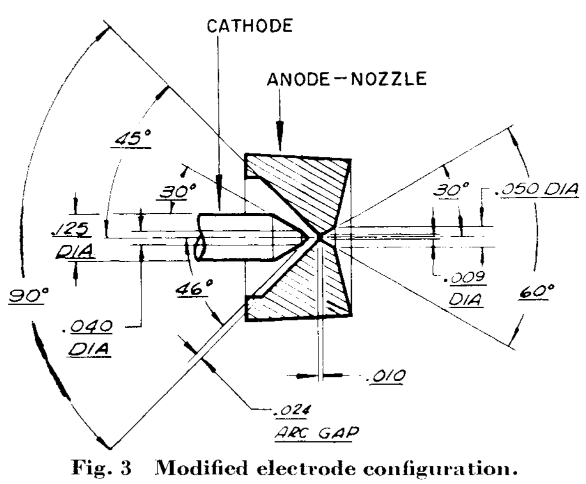

Fig. 3 Modified electrode configuration.

a low-pass filter that eliminated all signals above 0.2 cps and then into the recorder.

The thrust-beam calibrating assembly was independently supported from the top structure. After the cryogenic tank was filled and capped, and after the engine was mounted on the thrust beam, the mechanical zero of the system was positioned. During this process, the core of the Schaevitz differential transformer was placed so that an electrical zero was obtained. Once this was obtained and the recorder's galvonometer was positioned properly, calibration was accomplished by a dead-weight system.

The measuring system was adequate for most of the testing time, but occasionally the indicated thrust measurement drifted over a wide range, and it seemed that the system was sensitive to air movement. However, Daytronic amplifiers can become saturated and can drift when the transformer core movement is too large. Foundation vibrations also could have caused the drift. The thrust beam, represented schematically, can be considered to be a vibrometer that would faithfully measure all foundation frequency above 10 cps. Thus, when foundation vibrations were severe, drift occurred, and on several occasions negative thrust measurements were recorded. The accuracy of thrust measurement is believed to have been ±5% when the foundation was not vibrating.

Test Results and Discussion

The eight tests made at the Lewis facility are listed in Table 1. Only limited confidence can be placed in the specific impulse and efficiency results reported, because they directly involve the thrust measurements just described which were found to be sensitive to tank and foundation vibrations and to physical distortions in the vent and fill lines connected to the engine. Other parameters were more dependable, and a higher level of confidence could be placed in them. Estimated accuracies were: 1) pressure and temperature, ±1%; 2) mass flow, ±2%; 3) average d.c. power, ±1% (oscillations were neglected); and 4) thrust, the measuring system of which requires further development before an accuracy can be assigned. (A new thrust-measuring system has since been developed.[5])

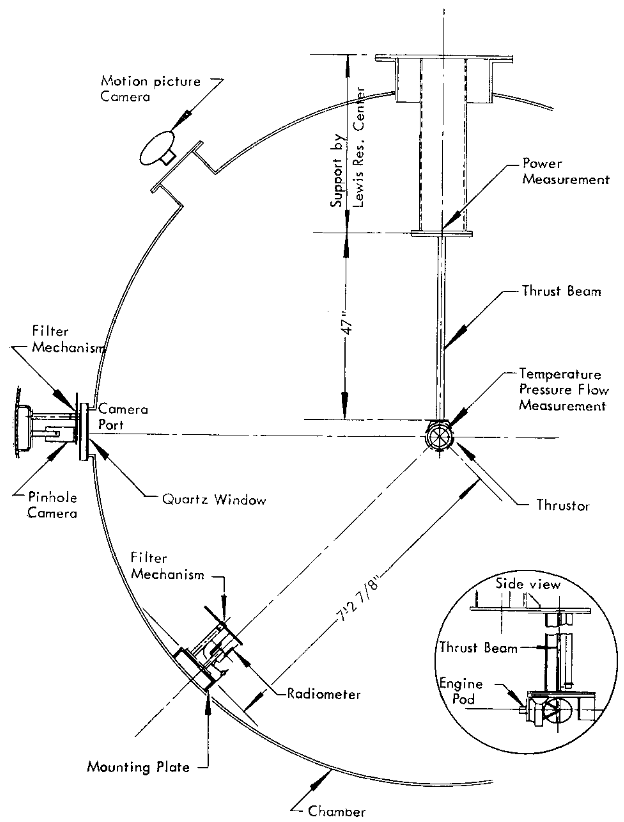

Fig. 4 Test setup.

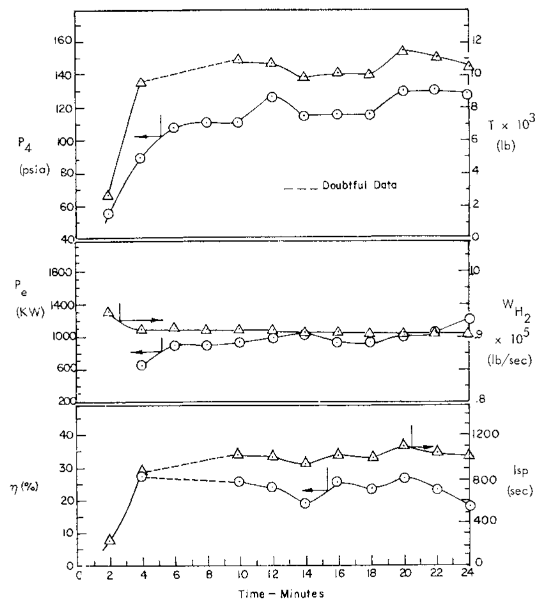

Fig. 5 Performance data vs time.

Plots of the data are presented in Figs. 5 and 6. Observations on these results and other data are as follows. Normally, the thrust and arc-chamber pressure should exhibit a consistent relationship if the gas constant, process constant, and nozzle geometry remain fixed over the range of gas temperatures achieved; Fig. 5 indicates that this relationship might exist. However, chamber pressure and thrust were not always in agreement; in many cases, the thrust values seem low. There is no way at present to establish whether thrust values were correct. Motion pictures of these tests show that severe nozzle ablation occurred simultaneously with drops in performance recorded on an oscillograph. Sudden drops in heating rates of the body also occurred with deterioration of performance. On one test, constant mass flow, arc chamber pressure, and power were maintained, but recorded thrust continuously decreased; this is believed to indicate errors in thrust determination.

Both the cathode and the anode were eroded (or ablated) during operation, but the most critical loss was at the nozzle throat (anode), where the area change directly affected the performance of the engine.

Prior to the testing, estimates of plume expansion for a hydrogen arcjet exhausting into ambient environments of 10^{-4} mm Hg and of 1 mm Hg were made. As a guide for the boundary approximations, E. K. Latvala's work[6] was used, and the values so determined were compared to photographs. During the tests, both color (Ektachrome) and high-speed IR photographs were taken. The latter were 2-min exposures through a fused silica window, whereas the former were taken at 24 frames/sec through a plate glass window. Each film then defined a jet boundary that was dependent on the spectral sensitivity of the film and absorption of the optics or windows

Table 1 Summary of arcjet-engine tests

Number of tests	Duration, min	Description
1	30	Varying power levels
3	30	At 1-kw power level
1	24	Planned flight schedule[1] of 24 min running followed by four stop-starts at ½–3-min intervals
1	24	Planned flight schedule followed by 100 stop-starts
2	24	Planned flight schedule

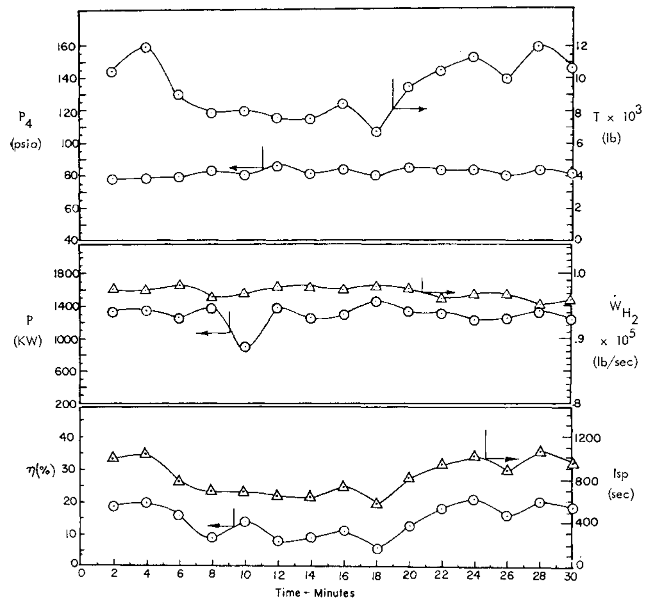

Fig. 6 Performance data vs time.

in the view. A comparison of the boundaries determined by these photographic methods with the calculated boundaries is given in Table 2. Figures 7a–7d show the boundaries of the jet at both pressures and under the conditions imposed by the pneumatic starter. Of importance is the fact that the boundary changes with power, arc-chamber pressure, and with the environmental pressure. Also notable is the fact that at 1-mm-Hg environmental pressure, no evidence of a blue outer fringe was found (Fig. 7d). Of interest are the following: 1) the plume suddenly appeared 1.13 sec after the cathode bellows chamber was retracted; the chamber pressure had by this time dropped significantly (see Fig. 8); 2) the plume was at first turned 18° above the thrustor's centerline (Fig. 7a), and then it slowly turned back to the centerline by the time the power was increased (Fig. 7c); 3) particles in the exhaust plume appeared to move along the centerline of the gas column, rather than the thrustor centerline (Fig. 7a);

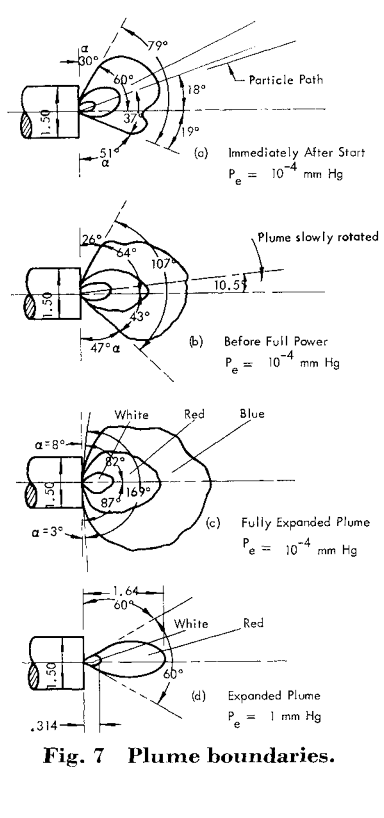

Fig. 7 Plume boundaries.

and 4) the visible plume boundary is affected by the arc-chamber pressure, power, and environmental pressure.

The objectives of the radiation measurements were to determine the absolute and relative intensities of the energy radiated in various spectral regions and to determine the spectral distribution. From the tests it is concluded that the total energy radiated from the plume was about 3–6% of input power. Most of the radiated energy appears to lie in the near uv and ir regions, with only a relatively small amount in the visible region (0.4–0.7 φ). Table 3 summarizes measurements taken during a typical test. Figure 9 shows a typical set of plume outlines.

By using the measured anode temperature and the assumed emissivity of molybdenum at operating conditions, estimates of the power radiated from the thrustor body can be made. Table 4 summarizes the significant data obtained.

Figure 8 is a copy of the Visicorder trace obtained from the start-stop operation during one of the tests. Figure 10 shows the time variations of four primary surface temperatures. Heating rates and final temperatures varied from test to

Table 2 Nozzle-turning angle vs pressure

Pressure, mm Hg	E. K. Latvala's approx.	Photographic method, av of 4 tests: Color movie	High-speed ir
1	60°	60°	67°
8×10^{-5}	23°	8°	31°

Table 3 Typical radiation data

Test conditions:	
Power, w	1283 (at 10.97 amp)
H_2 flow, lb/sec	0.97×10^{-5}
Vacuum chamber pressure, mm Hg	8×10^{-5}
I_{sp}, sec	833
Plume turning angle (deg)	28.5

Wavelength transmitted, μ	Source projected area, in.^{2}	Plume dimensions, in.: length	width	Energy radiated, w
0.19–4.0	33.6	5.6	7.8	36
0.76–4.25	4.7	2.1	3.7	19
0.24–0.40 0.68–0.87	10.3	3.0	5.2	16
0.39–0.87	19.5	3.4	4.1	9.5
0.36–0.38	0.9	1.1	1.2	4.1
0.38–0.40	5.3	2.1	3.9	7.0
0.87–1.6	...	...	...	6.8

Table 4 Estimates of radiated power

Test number (see Ref. 4)	Av radiation loss, w	Av current input, amp	Av power input, w	Approx. time to thermal equil., min	Input power radiated from body, %
1007	53	10.5	970	73	5.5
1009-I	81	8.9	1230	22	6.6
1009-II	68	11.0	1280	48	5.3
1009-III	80	11.3	1250	15	6.4
1010	74	10.6	1160	51	6.4

Table 5 Heat leak and hold time to pressurize tank

Tank number	Vol. eff., ft^3	Heat leak, Btu/hr	Hold time, hr: 450 psia	550 psia
A	0.0378	4.66	1.73	1.93
B	0.0373	2.65	2.45	2.86

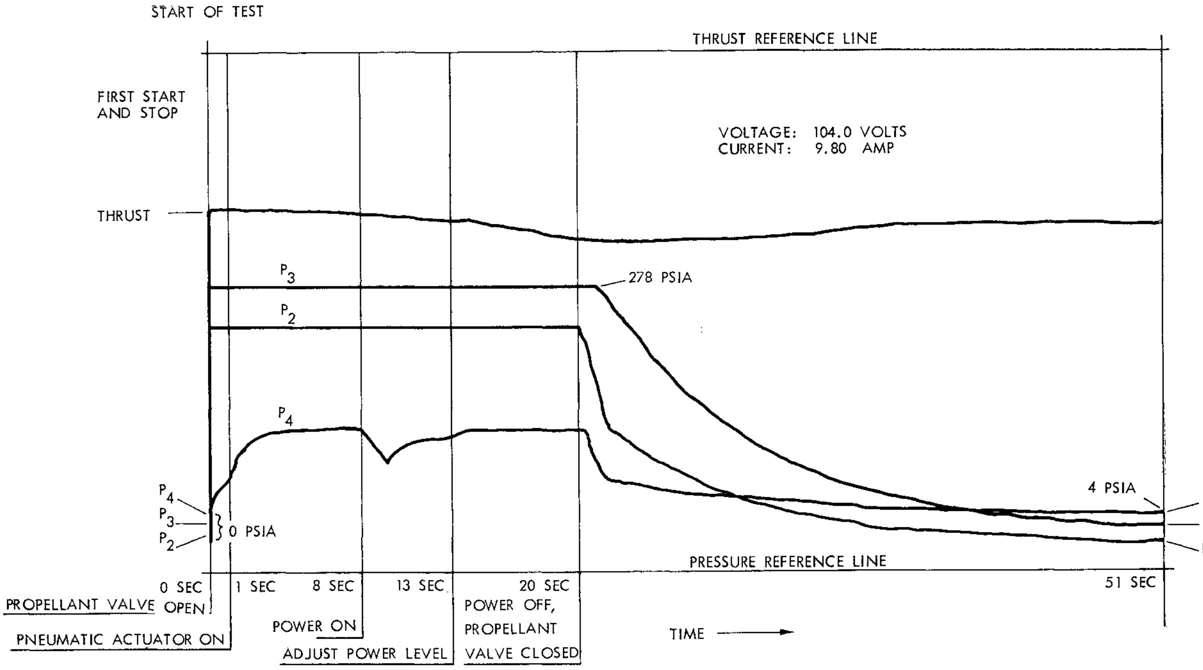

Fig. 8 First stop-start test results.

test. Since the thrustors were identical in size, weight, surface finish, and internal insulation, the variation in anode-temperature change rate (from 30°–100°F/min) can be attributed to changes in losses.

During the test program, three cryogenic tanks were delivered: two tanks of stainless steel and one of titanium. Titanium has advantages in higher strength-to-weight ratio and in lower thermal conductivity, but fabrication was difficult and expensive. The stainless-steel tanks performed adequately, but their ability to insulate degenerated over the five-month period.

Heat-leak rates were determined from the rate of change in internal energy for a closed tank containing supercritical hydrogen. The hydrogen charge weight, the effective volume of the tank, the pressure-time history, and thermodynamic data for 20.4° K equilibrium hydrogen[7] were used. To determine the effective volume of the tank, its actual volume was reduced by considering those parts of the tank and lines which contained hot gas (0.0019 ft^3) as 15% effective, since the warm volume will store only 15% as much fluid than it would if it were cold. Table 5 gives the heat leak and hold time as it existed prior to the thermal vacuum test.

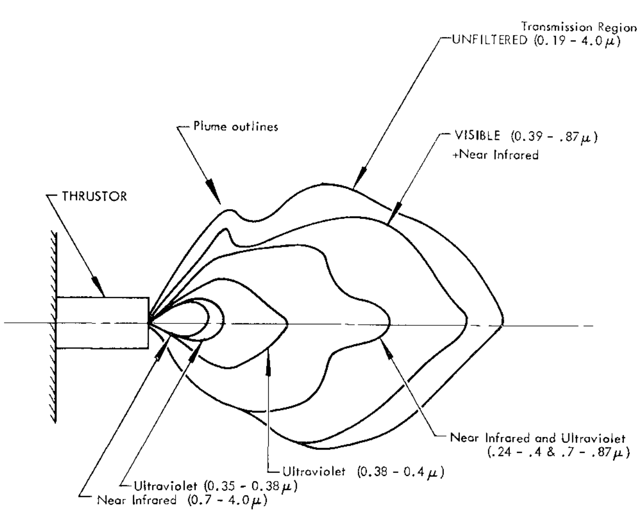

Fig. 9 Exhaust plumes of various spectral regions.

Conclusions and Recommendations

The arcjet engine operated satisfactorily for the flight-test sequence. However, performance values were of low reliability because of possible errors in the thrust and power measurement. The thrust-measuring system must be improved before further system tests seem warranted.

The engine was very reliable with respect to startup. No parts, except the nozzle throat, showed harmful deterioration.

The plume behaved essentially as could be predicted for low-pressure environments. About 5% of the input energy was lost in plume radiation, and 6% was lost by radiation from the thrustor body. The equilibrium surface temperature of the thrustor was between 2000° and 2500°R; heating rates were 55°R/min.

In view of the high-frequency oscillations, plume photographs should be made with a camera that includes a quartz

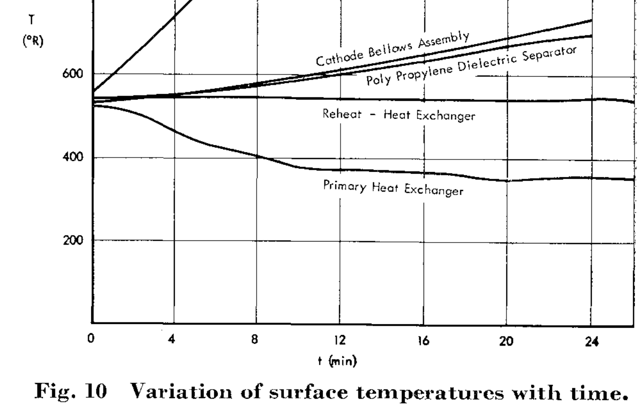

Fig. 10 Variation of surface temperatures with time.

lens in future tests. Film emulsions with a greater spectral sensitivity range should be sought. Use of a calibrated monochromator simultaneously with the thermopile radiometer would enable determination of a spectral distribution curve.

References

[1] Page, R. J. and Humpal, H. H., "The objectives and design of a 1 kw arc-jet engine for space flight testing," ARS Preprint 2346-02 (March 1962).

[2] Waltzer, H. and Brillhart, M., "Vacuum thermal balance test of 1 KW plasma arc engine," Plasmadyne Test Specification 101 (December 1961).

[3] Plasmadyne Staff, "The development of an electrothermal propulsion system," Plasmadyne Corp. Rept. PRE-101 (November 10, 1961).

[4] Ducati, A. C. and Muehlberger, E., "Study of an ignition system for hydrogen plasmajets," Plasmadyne Corp. Rept. no. PLR-118 (May 1962).

[5] Plasmadyne Staff, "Development of a plasmajet rocket engine for attitude and orbit control," Plasmadyne Final Rept. FR112-651, NASA Contract no. 5-651 (December 5, 1962).

[6] Latvala, E. K., "Spreading of rocket exhaust jets at high altitudes," ARO Project 100928, Contract AF 40(600)-700 S/A 13(59-1).

[7] Shaffer, A. and Rousseau, J., "Thermodynamic data for 20.4°K equilibrium hydrogen," Garrett Corp., AiResearch Div., ASD-TDR-61-360 (October 1961).